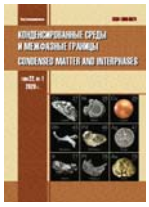

Condensed Matter and Interphases
(Kondensirovannye sredy i mezhfaznye granitsy)

Original articles

DOI: https://doi.org/10.17308/kcmf.2020.22/2507 eISSN 2687-0711
Received 24 January 2020
Accepted 15 February 2020
Published online 25 March 2020

The Composition and Structure of Phases, Formed in the Thermolysis of Substitutional Solid Solutions $H_2Sb_{2-x}V_xO_6 \cdot nH_2O$

© 2020 L. Yu. Kovalenko✉, V. A. Burmistrov, D. A. Zakhar'evich

Chelyabinsk State University,
129 Bratiev Kashirinykh str., Chelyabinsk 454001, Russian Federation

Abstract

In compounds, crystallized within the pyrochlore-type structure (sp.gr. Fd3m) of the $A_2B_2X_6X'$ general formula, there could be doubly or triply charged ions in the place of A cations, quadruply or quintuply charged ions in the place of B cations. Most works are devoted to the formation of these structures, depending on the nature and sizes of A and B cations, while little attention has been paid to determining the temperature ranges of their stability. The aim of this work was to study the thermolysis of substitutional solid solutions $H_2Sb_{2-x}V_xO_6 \cdot nH_2O$ in the range of 25–700 °C and the determination of the influence of the nature of B (Sb, V) cation on the stability of pyrochlore-type structures during heating.

Substitutional solid solutions have been obtained by the co-precipitation method. The samples, containing 0; 5 (x = 0.10); 15 (x = 0.30); 20 (x = 0.40); 24 (x = 0.48) at% of vanadium have been chosen as subjects of the present research. The changes in the proton hydrate sublattice in samples, containing different amounts of V^{+5} were analysed by IR spectroscopy. The modelling of the thermolysis process and determination of the phase compositions at each stage was possible using X-ray phase and thermogravimetric analysis of the samples

It was shown that at temperatures of 25–400 °C, proton-containing groups are removed from the hexagonal channels of the pyrochlore-type structure. The increase in number of V^{+5} ions in solid solutions changed the proton-binding energy with oxygen ions $[BO_3]^-$-octahedron, which led to the shift of stage boundaries: oxonium ions and water molecules were removed at higher temperatures, while hydroxide ions were removed at lower temperatures. An increase in temperature to over 500 °C led to the structure destruction due to the oxygen removal from $[BO_3]^-$-octahedrons. The model for the atomic filling of crystallographic positions in the pyrochlore-type structure for phases, formed during $H_2Sb_{2-x}V_xO_6 \cdot nH_2O$ thermolysis at 25–400 °C, has been proposed.

According to the thermogravimetric analysis, the structural formulas of solid solutions under the air-dry condition has been determined. $(H_3O)Sb_{2-x}V_xO_5(OH) \cdot nH_2O$, where $0 < x \le 0.48$, $0 < n \le 1.1$. It has been shown that the temperature ranges of thermolysis stages were affected by the proton-binding energy with oxygen ions $[BO_3]^-$-octahedron temperature ranges, where B = V, Sb, forming the structural frame. It has been found that the studied solid solutions are stable up to 400 °C within the framework of the pyrochlore-type structure.

Keywords: pyrochlore-type structure, antimony compounds, polyantimonic acid, substitutional solid solutions, thermal analysis, phase transformations.

Funding: The study was financially supported by the Russian Foundation for Basic Research (Grant no. 18-33-00269) and the Foundation for the Support of Young Scientists of Chelyabinsk State University.

For citation: Kovalenko L. Yu., Burmistrov V. A., Zakhar'evich D. A. The composition and structure of phases, formed in the thermolysis of $H_2Sb_{2-x}V_xO_6 \cdot nH_2O$ substitutional solid solutions. *Kondensirovannye sredy i mezhfaznye granitsy = Condensed Matter and Interphases*. 2020;22(2): 75–83. DOI: https://doi.org/10.17308/kcmf.2020.22/2507

✉ Liliya Yu. Kovalenko, e-mail: LKovalenko90@mail.ru

1. Introduction

Compounds crystallizing in pyrochlore-type structures with a general formula of $A_2B_2X_6X'$ have attracted the attention of scientists for more than fifty years [1–6]. The reason for this is elemental diversity. In the place of A cations there can be doubly or triply charged ions, in place of cations quadruply or quintuply charged ions, and as a result, the variety of properties of the pyrochlores: magnetic [7, 8], photocatalytic [9, 10], dielectric [11] and others. The authors have paid a lot of attention to the study of the formation of the structure depending on the radii of the ions and their arrangement in crystallographic site occupancies [1, 12, 13]. Thus, it was shown that such a structural type for compounds is preferable when the ratio of the radii A and B cations is: $1.46 \le r(A)/r(B) \le 1.61$ [12, 14]. For oxide systems in which oxygen atoms are located at site X, the most important in determining whether a pyrochlore-type structure will form are characteristics of $[BO_3]^-$-octahedrons [15]. However, little attention has been paid to studying the stability of compounds crystallizing in a pyrochlore-type structure during heating. The features of thermolysis were studied only for a few compounds [16–20].

In this work, we selected samples of polyantimonic acid (PAA) doped with vanadium ions, with $H_2Sb_{2-x}V_xO_6 \cdot nH_2O$ composition as a model system. When atoms are distributed over crystallographic site occupancies of a pyrochlore-type structure, the 8b positions remain vacant, in place of A cations, protons and oxonium ions are located, and Sb^{+5}, V^{+5} ions act as B cations [21]. As a result, a skeletal plane of a defective structure is formed, consisting of $[BO_3]^-$-octahedrons connected by apexes and having hexagonal channels in which protons, oxonium ions, and water molecules are located. Doping of PAA with V^{+5} ions leads to a change in the binding energy of protons with $[BO_3]^-$ and, as a consequence, an increase in proton conduction [22].

According to studies [23–25], proton-containing groups located in the channels of the structure have a significant influence on the stabilization of the PAA phase at high temperatures. Therefore, the doping of PAA with V^{+5} ions should change the phase stability during heating. Therefore, the aim of this work was to study the thermolysis of $H_2Sb_{2-x}V_xO_6 \cdot nH_2O$ substitutional solid solutions in the temperature range of 25–700 °C, the determination of the composition and structure of phases at each stage of thermolysis, the determination of the influence of the nature of B (Sb, V) cation on the stability of pyrochlore-type structure during heating.

2. Experimental

Samples were synthesized by coprecipitation of solutions of sodium vanadate and antimony trichloride, pre-oxidized with nitric acid, in an excess of distilled water according to the procedure described in the study [21]. The resulting precipitate was separated from the mother liquor, washed with distilled water until the negative reaction of filtrate to chlorine ions, dried in air, and kept at room temperature for a long time under normal conditions (T = 25 °C, RH ≈ 60 %). All chemicals used were of analytical grade.

Ratios of vanadium and antimony (at%) in the samples were determined based on the data of ARL QuanT'X X-ray fluorescence spectrometer, device sensitivity <1 ppm.

In previous studies [21, 26], it was shown that, within the framework of the pyrochlore type structure, a substitutional solid solution $H_2Sb_{2-x}V_xO_6 \cdot nH_2O$ is formed at $0 < x \le 0.48$. Therefore, finely dispersed powders containing according to elemental analysis 0; 5 (x = 0.10); 15 (x = 0.30); 20 (x = 0.40); 24 (x = 0.48) at% vanadium were selected as objects of study.

The IR absorption spectra of the samples were recorded on a Nicolet 380 IR Fourier spectrometer in the frequency range from 500 to 4000 cm^{-1}. For this, the samples were mixed with KBr powder and pounded to a finely dispersed state, followed by pressing the mixture in a compressing mould. As the result, a translucent tablet was obtained.

Phase samples at different stages of thermolysis were obtained by prolonged heat treatment of solid solutions in air at temperatures 400 and 650 °C.

Structural studies of the initial and heat treated samples were performed on a Rigaku Ultima IV X-ray diffractometer (filtered Cu$K\alpha$-radiation) in the range of diffraction angles $10 \le 2\theta \le 70$ deg.

Thermal studies of the samples were carried out using Netzsch STA 449F5 Jupiter synchronous

thermal analyser in air. We recorded the change in the mass of the sample and rate of its change during heating at 10 °C/min in the temperature range 24–700 °C, the balance sensitivity was 100 mg. Samples were weighed on an analytical balance with an accuracy of 0.0001 g before and after heating.

For a quantitative assessment of the thermal decomposition of the samples, the relative mass change was found $\Delta\mu_{ТГ}$:

$$\Delta\mu_{ТГ} = \frac{\Delta m_i}{\Delta m_k}, \quad (1)$$

where Δm_i – mass change at the given thermal decomposition stage, Δm_k – mass of the final product.

Based on the amount of removed products at each stage, the process of thermolysis of solid solutions was simulated. For the validation of the selected model, the relative mass change of the samples was found $\Delta\mu_T$:

$$\Delta\mu_T = \frac{\Delta M_{ri}}{\Delta M_{rk}}, \quad (2)$$

where ΔM_{ri} – change in the molecular mass of the thermolysis product at given stage of thermal decomposition, ΔM_{rk} –molecular mass of the final decomposition product - a mixture of two phases $Sb_2O_{4.3\,(4)}$ and $VSbO_4$ taking into account the given V/Sb ratio. The model was selected in a way, that the discrepancy between $\Delta\mu_{ТГ}$ and $\Delta\mu_T$ was the lowest.

3. Results and discussion

Substantial doping of PAA crystallizing in the pyrochlore type structure should lead to a change in the structure of the protohydrate sublattice while maintaining the charge of the main frame [21, 22].

On the IR spectra of PAA and doped forms, a wide complex absorption band in the region of 3700–2700 cm^{-1} (Fig. 1) can be distinguished, which corresponds to the vibrations of hydroxide ions and water molecules involved in the νO–H hydrogen bond [24, 27, 28]. Two maxima can be detected in this region (Fig. 1): at 3400 cm^{-1}, which is attributed to the vibrations of molecules of loosely bound water, and 3250 cm^{-1} responsible for the vibrations of hydroxide ions and water molecules perturbed by the surface field of the crystal lattice [29–31].

The absorption band at 3250 cm^{-1} with an increasing amount of V^{+5} shifts to the region of lower frequencies (Fig. 1). Thus, for the saturated solid solution (x = 0.48) the maximum band has a value of 3200 cm^{-1} (Fig. 1). According to studies [28, 32, 33], the shift of the frequency of stretching vibrations of hydroxide ions to the low frequencies (red shift of collective symmetric vibrations) upon formation of hydrogen bond was due to a decrease in the force constant of the O–H bond itself. Therefore, doping of PAA with V^{+5} ions reduces the energy of interaction of protons with oxygen anions of $[BO_3]^-$-octahedron and, as a result, leads to the weakening of hydrogen bonds in the hexagonal channels of the structure.

In the region of deformation vibrations, intense absorption bands were recorded on the spectra at 1400, 1640 cm^{-1}, corresponding to deformation

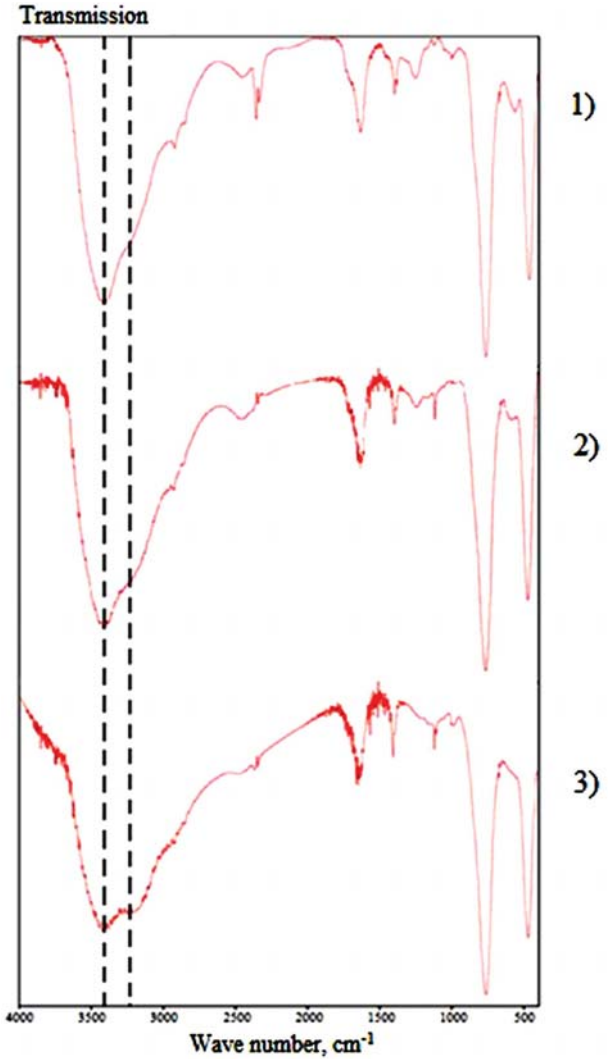

Fig. 1. IR spectra of samples $H_2Sb_{2-x}V_xO_6 \cdot nH_2O$, where x: 0 (*1*); 0.10 (*2*); 0.48 (*3*)

vibrations δ (Sb^{+5}-OH) and deformation vibrations of water molecules, respectively (Fig. 1) [24, 27]. Band intensity at 1700 cm^{-1}corresponding to deformation vibrations of oxonium ions with increasing amount of V^{+5} decreases. The region of deformation vibrations was less sensitive to the formation of hydrogen bonds of different strengths than the region of stretching vibrations; therefore, a shift of the bands of deformation vibrations to the low-frequency region was not observed (Fig. 1) [28, 34].

Absorption bands at 770 and 450 cm^{-1} corresponded to the stretching vibrations of ν (Sb^{+5}–O). For doped forms, the appearance of additional absorption bands corresponding to V–O bonds was not observed [35]. The absence of additional bands confirms the similarity of the fingerprint region of V–O and Sb–O bonds in complex oxides.

According to thermogravimetric analysis of $H_2Sb_{1.52}V_{0.48}O_6 \cdot nH_2O$ sample, broad maxima can be distinguished on the mass change rate curve at temperatures of 140 (stages I and II), 280 (stage III) and 560 (stage V) °C (Fig. 2). According to published data [24], in the 100 °C region, during the thermolysis of hydrated oxides and acids adsorbed water molecules should be removed (stage I), and at higher temperatures (100–200 °C) water molecules located near the crystal lattice (stage II) should be removed. It was believed that the first broad maximum reflects the superposition of stages I and II (Fig. 2). With an increase in the amount of V^{+5} in solid solution, the maximum in the mass change rate curve at 400 °C shifted to the region of lower temperatures, its intensity decreased (Fig. 3). However, according to the TG curve (Fig. 2), mass loss was observed in this temperature range (stage IV). For the clarification of the thermolysis stages, an X-ray phase analysis of samples heat treated at temperatures of 400 and 650 °C was carried out.

On the X-ray diffraction patterns of $H_2Sb_{1.52}V_{0.48}O_6 \cdot nH_2O$ sample after heat treatment at 400 °C (Fig. 4), the lines became of low-intensity, however, the position of the reflections coincided with the initial X-ray diffraction pattern.

Reflections with odd indices extinguished and it was also observed for the undoped PAA sample [24], and indicated the dehydration of compounds and the rearrangement of the structure [23, 24, 34]. In the temperature range 500–600 °C, the decomposition of compounds and the formation of two phases, one of which was $Sb_2O_{4.3(4)}$, the other – $VSbO_4$ phase with the crystal structure of the rutile type (sp. gr. $P4_2/mnm$) was observed [36, 37].

According to the data of a full-profile X-ray analysis [26] carried out for $H_2Sb_{2-x}V_xO_6 \cdot nH_2O$, $0 < x \leq 0.48$ solid solutions, Sb^{+5} and V^{+5} ions and were statistically located at the 16c positions and formed $[BO_3]$-octahedrons with oxygen anions and hydroxyl groups occupying the 48f positions. Oxonium ions and water molecules statistically

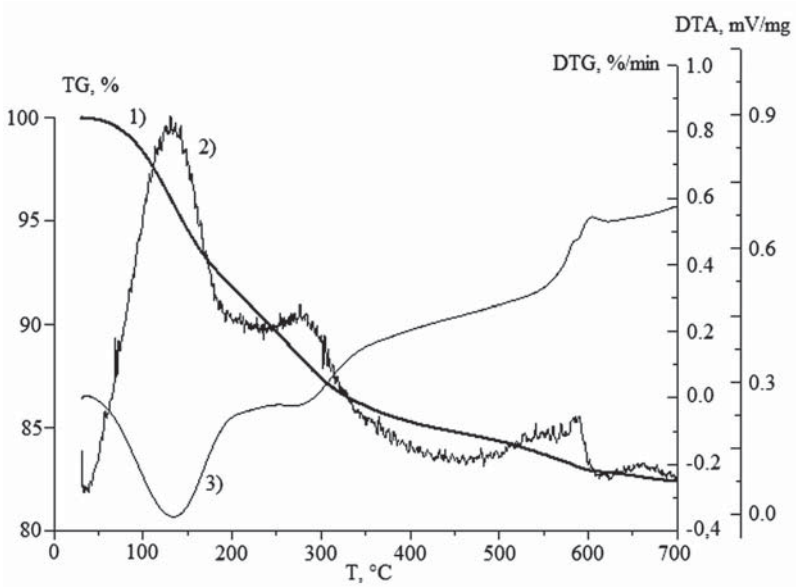

Fig. 2. Dependences of the change in mass – TG (*1*), the rate of change in mass – DTG *(2)* and the change in heat flux – DTA (*3*) of the $H_2Sb_{1.52}V_{0.48}O_6 \cdot nH_2O$ sample on temperature

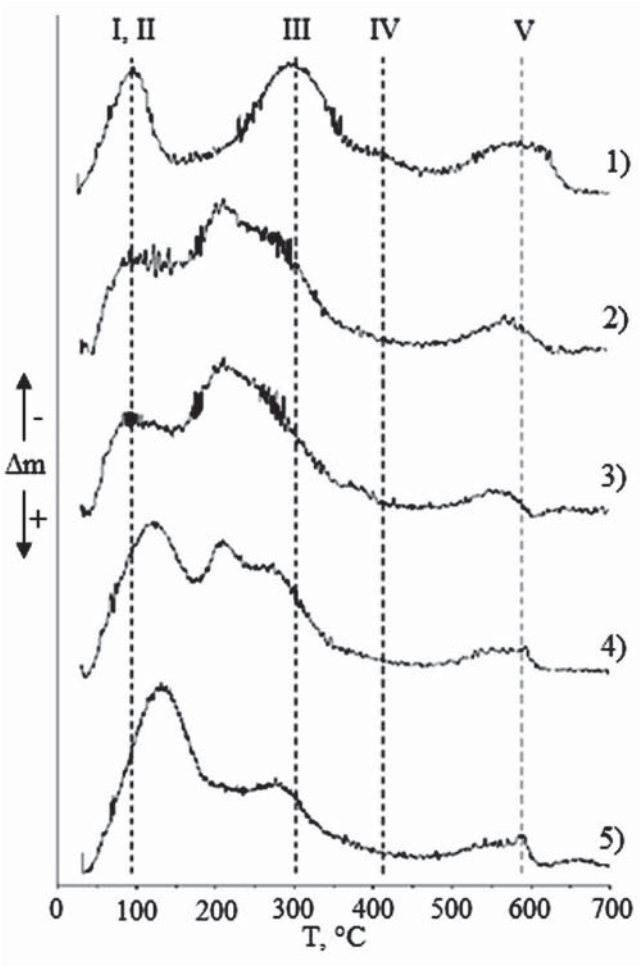

Fig. 3. Dependences of the rate of change of mass (DTG) on the temperature of samples $H_2Sb_{1.52}V_{0.48}O_6 \cdot nH_2O$, in which x: 0 (*1*); 0.10 (*2*); 0.30 (*3*); 0.40 (*4*); 0.48 (*5*); Roman numerals I–V indicate stage numbers

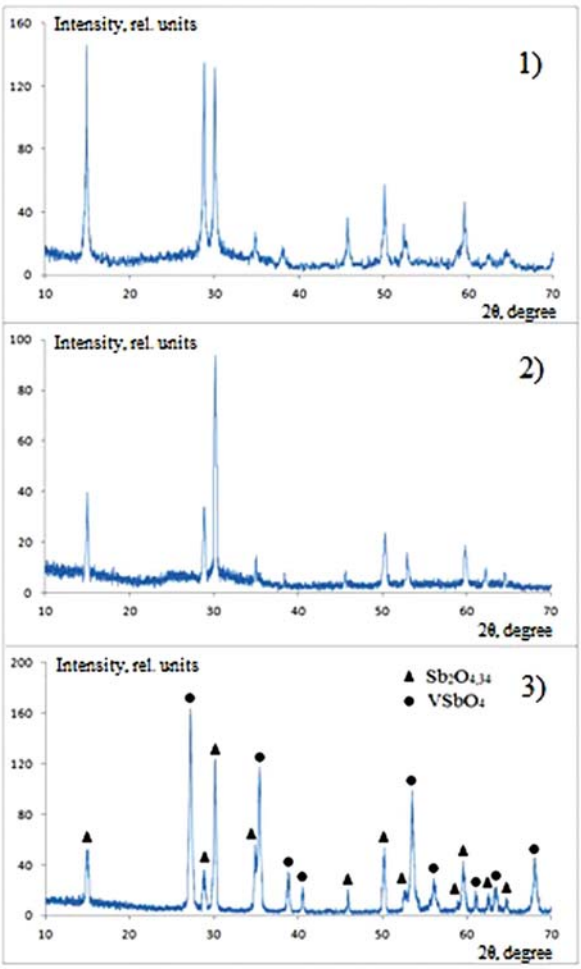

Fig. 4. X-ray diffraction patterns of $H_2Sb_{1.52}V_{0.48}O_6 \cdot nH_2O$ (*1*) and phases formed after heating at 400 °C (*2*) and 650 °C (*3*)

filled the 16d positions and were located in hexagonal channels. The change in the X-ray pattern at temperatures above 500 °C was due to the removal of protons from the 16d positions of the structure and the transition of Sb^{+5} and V^{+5} ions from octahedral into cubic positions [24]. Thus, the substitutional solid solutions $H_2Sb_{2-x}V_xO_6 \cdot nH_2O$ within the pyrochlore-type structure were stable up to 400 °C.

For the determination of the phase composition at different stages of thermolysis, we used the following assumption [24]: during thermal transformations, the number of antimony and vanadium atoms does not change, water and oxygen molecules are removed in different temperature ranges. According to mass spectrometry data [24], in the temperature range 24 - 500 °C water molecules (18 a.m.u.) were removed, and in the range of 500 - 700 °C oxygen molecules (32 a.m.u.) were removed. The calculations of the relative mass change were carried out using equations 1 and 2, the results are presented in Table 1.

The experimental and calculated values of the mass loss were in good agreement (Table 1) indicating a correct description of the thermolysis stages. Thus, we were able to determine the initial composition of the solid solution $(H_3O)Sb_{1.52}V_{0.48}O_5(OH) \cdot 0.4H_2O$, its formation temperature and phase composition at each stage of thermolysis. The model of the distribution of atoms over the crystallographic site occupancies of a pyrochlore-type structure for phases formed at temperatures 25-400 °C is presented in Table 2. Water molecules, weakly bound to the structure, were statistically located at 8b positions.

During stages I and II of thermolysis, adsorbed water and water molecules were removed from the

Table 1. The stages of thermolysis of $(H_3O)Sb_{1.52}V_{0.48}O_5(OH)\cdot 0.4H_2O$, according to the proposed model, where $\Delta\mu_t$ – relative changes in the mass of the doped sample; $\Delta\mu_{TG}$ – experimental mass values according to the TG data, relative to the final mass of the sample; temperature ranges ΔT of the stages of phase formation

Stage no.	Reaction	Stage temperature range ΔT, °C	$\Delta\mu_T$, %	$\Delta\mu_{TG}$, %
I–II	$(H_3O)Sb_{1.52}V_{0.48}O_5(OH)\cdot 0.4H_2O = (H)Sb_{1.52}V_{0.48}O_5(OH) + 1.4H_2O$	24–190	9.11	9.37
III	$(H)Sb_{1.52}V_{0.48}O_5(OH) = Sb_{1.52}V_{0.48}O_{4.5}(OH) + 0.5H_2O$	200–300	3.25	3.16
IV	$Sb_{1.52}V_{0.48}O_{4.5}(OH) = Sb_{1.52}V_{0.48}O_5 + 0.5H_2O$	300–360	3.25	3.48
V	$Sb_{1.52}V_{0.48}O_5 = 0.52Sb_2O_{4.3(4)} + 0.48VSbO_4 + 0.41O_2$	520–600	4.74	4.57
	TOTAL:	24–600	20.35	20.58

Table 2. The distribution of atoms according to the crystallographic positions of a pyrochlore type structure for $(H_3O)Sb_{1.52}V_{0.48}O_5(OH)\cdot 0.4H_2O$ and phases formed upon heating (number of formula units Z = 8)

Stages	Formation temperature , °C	Structural formula	16d	16c	48f	8b
–	25	$(H_3O)_8Sb_{12}V_4O_{40}(OH)_8\cdot 3.2H_2O$	$8H_3O^+$	$12Sb^{+5}$, $4V^{+5}$	40 O^{-2} 8 OH^-	$3.2H_2O$
I–II	190	$(H)_8Sb_{12}V_4O_{40}(OH)_8$	$8H^+$	$12Sb^{+5}$, $4V^{+5}$	40 O^{-2} 8 OH^-	–
III	260	$(Sb^{+5})_2Sb_{12}V_4O_{40}(OH)_8$	$2Sb^{+5}$	$12Sb^{+5}$, $4V^{+5}$	40 O^{-2} 8 OH^-	–
IV	360	$(Sb^{+5})_4Sb_{12}V_4O_{48}O_2$	$4Sb^{+5}$	$12Sb^{+5}$, $4V^{+5}$	48 O^{-2}	$2O^{-2}$

16d positions. In the resulting $(H)_8Sb_{12}V_4O_{40}(OH)_8$ phase the $[BO_3]^-$ negative charge was compensated by protons located in the 16d positions. Further heating led to the destruction of the octahedrons due to the interaction of protons located in the 16d positions with part of the oxygen anions of the $[BO_3]^-$-octahedron. In this case, part of the Sb^{+5} ions passed from the 16c into the 16d positions (Table 2). In the phase forming during stage III $(Sb^{+5})_2Sb_{12}V_4O_{40}(OH)_8$ Sb^{+5} ions are compensated by the charge of $[BO_3]^-$-octahedrons. During stage IV, hydroxyl groups were removed in the form of water molecules, octahedrons were further destroyed, and further transitions of Sb^{+5} ions from the 16c into the 16d positions occurred. The $(Sb^{+5})_4Sb_{12}V_4O_{48}O_2$ phase was stable due to Sb^{+5} ions located in the 16d positions. At temperatures above 500 °C, the removal of oxygen began, which indicated the reduction of part of the Sb^{+5} ions into Sb^{+3} and the destruction of the structure.

The removal of proton-containing groups during stages I–III was characterized by endo-effects, the minima of which in the curves of the heat flux (DTA) were fixed at 140 and 290 °C (Fig. 2). With further heating, a small maximum at 320 °C was recorded: the formation of the $(Sb^{+5})_4Sb_{12}V_4O_{48}O_2$ phase was accompanied by heat production. At 600 °C, the exo-effect was associated with the formation of two new phases, $Sb_2O_{4.3(4)}$ and $VSbO_4$.

For solid solutions in which $x < 0.48$, the same number of stages was fixed during thermolysis (Fig. 3), the mass loss was from 18 to 22 % relative to the final decomposition products. With an increase in the amount of vanadium, a substitutional solid solution $(H_3O)Sb_{2-x}V_xO_5(OH)\cdot nH_2O$ contained lower amount of water in an air-dry state. Thus, according to thermogravimetric analysis, $n = 0.4$ for the saturated substitutional solid solution ($x = 0.48$), $n = 1.1$ for PAA [24].

On the mass change rate curves (DTG) of the doped samples, the shift of the stage maxima with an increase in the amount of dopant was recorded (Fig. 3). The maxima of I and II stages were shifted to the region of high temperatures, for the saturated solid solution from 95 to 140 °C. The maxima of stages III and IV, on the contrary, shifted to the low-temperature region. The shift from 300 to 270 °C and 400 to 370 °C respectively was revealed for the saturated solid solution. The shift of stages I and II was probably due to the removal of proton-containing groups at higher temperatures and the higher bonding force of the protonhydrate lattice with the crystal lattice.

The shift of the maxima of stages III and IV into the low temperature region was a common characteristic of doped oxides and heteropoly acids. Probably, the introduction of vanadium facilitates the transition of neighbouring atoms or ions from the main positions into the excited state, according to the order-disorder theory, lowers the decomposition temperature [38].

Stage shifts were also recorded on the curves of heat flux (DTA curves). With an increase in the amount of V^{+5}, the removal of oxonium ions from the 16d positions (stage I and II) occurred at higher temperatures and was accompanied by high energy costs, as was evidenced by the large minimum area at temperatures of 100–150 °C (Fig. 5). The transition of Sb^{+5} ions from the 16c to 16d positions, on the contrary, was more beneficial (Fig. 5, stages III and IV). Thus, the endothermic minimum of stage III (300 °C) shifted to the lower temperature region and its area decreased. The exothermic maximum (370 °C), indicating the formation of the $Sb_{2-x}V_xO_5$ phase shifted to the low-temperature region with an increasing amount of V^{+5} in the solid solution. In the high-temperature region, an exothermic peak (600–630 °C) of high intensity appeared, associated with the formation of two new phases – $Sb_2O_{4.3(4)}$ and $VSbO_4$.

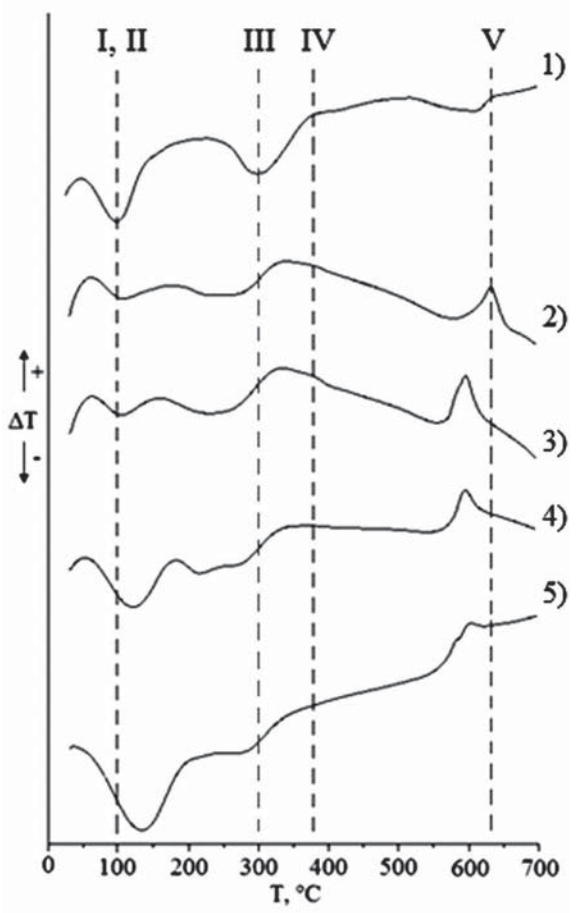

Fig. 5. Dependences of the change in heat flux (DTA) on the temperature of samples $H_2Sb_{2-x}V_xO_6 \cdot nH_2O$, where x: 0 (*1*); 0.10 (*2*); 0.30 (*3*); 0.40 (*4*); 0.48 (*5*)

Due to the electronic structure of the vanadium ion, the O–V bond is less covalent than the O–Sb bond [39]; therefore, the proton must form a stronger bond with the oxygen ion of the $[VO_3]^-$ octahedron, which was confirmed by the DTG and DTA data, which showed the shift of stages I and II to the high-temperature region (Fig. 3, Fig. 5). Changes in the binding energy between protons located in hexagonal channels and oxygen ions of $[BO_3]^-$-octahedrons affected the transport of protons between electronegative atoms. As a result, the distance between protons and oxygen ions of $[SbO_3]^-$-octahedrons increased, and the red shift of νO–H vibrations of hydroxide ions and water molecules was recorded on the IR-spectra (Fig. 1). High proton mobility led to an increase in proton conductivity with an increase in the amount of vanadium in the samples [22].

4. Conclusions

It was found that the resulting solid solutions have the structural formulas $(H_3O)Sb_{2-x}V_xO_5(OH) \cdot nH_2O$, where $0 < x \leq 0.48$, $0 < n \leq 1.1$. Doping leads to a change in the proton-binding with oxygen ions $[BO_3]^-$-octahedrons, where B = V, Sb, forming the structural frame, changing the temperature ranges of the thermolysis stages. It has been shown that substitutional solid solutions $H_2Sb_{2-x}V_xO_6 \cdot nH_2O$ within a framework of the pyrochlore-type structure were stable up to 400 °C. The model describing the sequence of phase transformations during the thermolysis of substitutional solid solutions $H_2Sb_{2-x}V_xO_6 \cdot nH_2O$ in the temperature range 25–400 °C was proposed, the composition of the phases during each thermolysis stage was established.

Acknowledgements

The study was supported by the Foundation for the Support of Young Scientists of Chelyabinsk State University.

Conflict of interests

The authors declare that they have no known competing financial interests or personal

relationships that could influence the work reported in this paper.

References

1. Subramanian M. A., Aravamudan G., Rao G. V. S. Oxide pyrochlores – A review. *Progress in Solid State Chemistry*. 1983;15(2): 55–143. DOI: https://doi.org/10.1016/0079-6786(83)90001-8

2. Krasnov A. G., Piir I. V., Koroleva M. S., Sekushin N. A., Ryabkov Y. I., Piskaykina M. M., Sadykov V. A., Sadovskaya E. M., Pelipenko V. V., Eremeev N. F. The conductivity and ionic transport of doped bismuth titanate pyrochlore $Bi_{1.6}M_xTi_2O_{7-\delta}$ (M – Mg, Sc, Cu). *Solid State Ionics*. 2017;302: 118–125. DOI: https://doi.org/10.1016/j.ssi.2016.12.01.019

3. Cherednichenko L. A., Moroz Ya. A. Catalytic properties of heteropolytungstates with 3d elements and their thermolysis products. *Kinetics and Catalysis*. 2018;59(5): 572–577. DOI: https://doi.org/10.1134/S0023158418050038

4. Krasnov A. G., Kabanov A. A., Kabanova N. A., Piir I. V., Shein I. R. Ab initio modeling of oxygen ion migration in non-stoichiometric bismuth titanate pyrochlore $Bi_{1.5}Ti_2O_{6.25}$. *Solid State Ionics*. 2019;335: 135–141. DOI: https://doi.org/10.1016/j.ssi.2019.02.023

5. Farlenkov A. S., Khodimchuk A. V., Eremin V. A., Tropin E. S., Fetisov A. V., Shevyrev N. A., Leonidov I. I., Ananyev M. V. Oxygen isotope exchange in doped lanthanum zirconates. *Journal of Solid State Chemistry*. 2018;268: 45–54. DOI: https://doi.org/10.1016/j.jssc.2018.08.08.022

6. Rejith R. S., Thomas J. K., Solomon S. Structural, optical and impedance spectroscopic characterizations of $RE_2Zr_2O_7$ (RE = La, Y) ceramics. *Solid State Ionics*. 2018;323: 112–122. DOI: https://doi.org/10.1016/j.ssi.2018.05.025

7. Egorysheva A. V., Ellert O. G., Gaitko O. M., Berseneva A. A., Maksimov Y. V., Dudkina T. D. Magnetic properties of $Pr_{2-x}Fe_{1+x}SbO_7$ and $Bi_{2-x}Ln_xFeSbO_7$ (Ln = La, Pr) pyrochlore solid solutions. Inorganic Materials. 2016;52(10): 1035-1044. DOI: https://doi.org/10.1134/S0020168516100071

8. Rau J. G., Gingras M. J. P. Frustrated quantum rare-earth pyrochlores. *Annual Review of Condensed Matter Physics*. 2019;10(1): 357–386. DOI: https://doi.org/10.1146/annurev-conmatphys-022317-110520

9. Lomanova N. A., Tomkovich M. V., Sokolov V. V., Ugolkov V. L. Formation and thermal behavior of nanocrystalline $Bi_2Ti_2O_7$. *Russian Journal of General Chemistry*. 2018;88(12): 2459–2464. DOI: https://doi.org/10.1134/s1070363218120010

10. Liu X., Huang L., Wu X., Wang Z., Dong G., Wang C., Liu Y., Wang L. $Bi_2Zr_2O_7$ nanoparticles synthesized by soft-templated sol-gel methods for visible-light-driven catalytic degradation of tetracycline. *Chemosphere*. 2018;210: 424–432. DOI: https://doi.org/10.1016/j.chemosphere.2018.07.040

11. Weller M. T., Hughes R. W., Rooke J., Knee Ch. S., Reading J. The pyrochlore family - a potential panacea for the frustrated perovskite chemist. *Dalton transactions*. 2004;19: 3032–3041. DOI: https://doi.org/10.1039/B401787K

12. Knop O., Brisse F., Meads R. E., Brainbridge J. Pyrochlores. IV. Crystallographic and Mossbauer studies of A_2FeSbO_7 pyrochlores. *Canadian Journal of Chemistry*. 1968;46: 3829–3832. DOI: https://doi.org/10.1139/v68-635

13. Sadykov V. A., Koroleva M. S., Piir I. V., Chezhina N. V., Korolev D. A., Skriabin P. I., Krasnov A. V., Sadovskaya E. M., Eremeev N. F., Nekipelov S. V., Sivkov V. N. Structural and transport properties of doped bismuth titanates and niobates. *Solid State Ionics*. 2018;315: 33–39. DOI: https://doi.org/10.1016/j.ssi.2017.12.00.008

14. Egorysheva A. V., Popova E. F., Tyurin A. V. Khoroshilov A. V., Gajtko O. M., Svetogorov R. D. Complex rare-earth tantalates with pyrochlore-like structure: synthesis, structure, and thermal properties. *Russian Journal of Inorganic Chemistry*. 2019;64: 1342–1353. DOI: https://doi.org/10.1134/S0036023619110056

15. McCauley R. A. Structural characteristics of pyrochlore formation. *Journal of Applied Physics*. 1980;51(1): 290–294. DOI: https://doi.org/10.1063/1.327368

16. Lupitskaya Y. A., Burmistrov V. A. Phase formation in the K_2CO_3-Sb_2O_3-WO_3 system on heating. *Russian Journal of Inorganic Chemistry*. 2011;56(2): 290–292. DOI: https://doi.org/10.1134/S0036023611020173

17. Piir I. V., Koroleva M. S., Korolev D. A., Chezina N. V., Semenov V. G., Panchuk V. V. Bismuth iron titanate pyrochlores: Thermostability, structure and properties. *Journal of Solid State Chemistry*. 2013;204: 245–250. DOI: https://doi.org/10.1016/j.jssc.2013.05.031

18. Lupitskaya Y. A., Kalganov D. A., Klyueva M. V. Formation of compounds in the Ag_2O–Sb_2O_3–MoO_3 system on heating. *Inorganic materials*. 2018;54(3): 240–244. DOI: https://doi.org/10.1134/S0020168518030081

19. Lomakin M. S., Proskurina O. V., Danilovich D. P., Panchuk V. V., Semenov V. G., Gusarov V. V. Hydrothermal synthesis, phase formation and crystal chemistry of the pyrochlore/Bi_2WO_6 and pyrochlore/α-Fe_2O_3 composites in the Bi_2O_3–Fe_2O_3–WO_3 system. *Journal of Solid State Chemistry*. 2020,282: 121064 DOI: https://doi.org/10.1016/j.jssc.2019.121064

20. Yang J., Han Y., Shahid M., Pan W., Zhao M., Wu W., Wan C. A promising material for thermal barrier coating: Pyrochlore-related compound Sm_2FeTaO_7. *Scripta Materialia*. 2018;149: 49–52. DOI: https://doi.org/10.1016/j.scriptamat.2018.02.005

21. Kovalenko L. Yu., Burmistrov V. A., Lupitskaya Yu. A., Kovalev I. N., Galimov D. M. Synthesis of

the solid solutions $H_2Sb_{2-x}V_xO_6 \cdot nH_2O$ with the pyrochlore-type structure *Butlerovskie soobshhenija = Butlerov Communications*. 2018;55(8): 24–30. ROI: jbc-01/jbc-01/18-55-8-24 (In Russ., abstract in Eng.)

22. Kovalenko L. Yu., Burmistrov V. A. Dielectric relaxation and proton conductivity of polyantimonic acid doped with vanadium ions. *Kondensirovannye sredy i mezhfaznye granitsy = Condensed Matter and Interphases*. 2019;21(2): 204–214. DOI: https://doi.org/10.17308/kcmf.2019.21/758 (In Russ., abstract in Eng.)

23. Trofimov V. G., Sheinkman A. I., Kleshchev G. V. About antimony pentoxide in a crystalline state. *Journal of Structural Chemistry*. 1973;14(2): 275–279. (In Russ.)

24. Kovalenko L. Yu., Yaroshenko F. A., Burmistrov V. A., Isaeva T. N., Galimov D. M. Thermolysis of Hydrated Antimony Pentoxide. *Inorganic Materials*. 2019;55(6): 586–592. DOI: https://doi.org/10.1134/S0020168519060086

25. Chen J., Chen Z., Zhang X., Li X., Yu L., Li. D. Antimony oxide hydrate ($Sb_2O_5 \cdot 3H_2O$) as a simple and high efficient photocatalyst for oxidation of benzene. *Applied Catalysis B: Environmental*. 2018;210: 379–385. DOI: https://doi.org/10.1016/j.apcatb.2017.04.004

26. Kovalenko L. Yu., Burmistrov V. A., Lupitskaya Yu. A., Yaroshenko F. A., Filonenko E. M., Bulaeva E. A. Ion exchange of H^+/Na^+ in polyantimonic acid, doped with vanadium ions. *Pure and Applied Chemistry*. 2019. DOI: https://doi.org/10.1515/pac-2019-0112

27. Yukhnevich G. V. Advances in the use of infrared spectroscopy for the characterization of OH bonds. *Russian Chemical Reviews*. 1963;32(11): 619–633. DOI: https://doi.org/10.1070/RC1963v032n11ABEH001370

28. Tarasova N. A., Animitsa I. E. The influence of the nature of halogen on the local structure and intercalation of water in oxyhalides Ba_2InO_3X (X = F, Cl, Br). *Optics and Spectroscopy*. 2018;124: 163. DOI: https://doi.org/10.1134/S0030400X18020170

29. Deryagin B. V., Churaev N. V., Ovcharenko F. D., Tarasevich Ju. I., Bukin V. A., Sarvazjan A. P., Harakoz D. P., Saushkin V. V. *Water in disperse systems*. Moscow: Chemistry Publ.; 1989. 288 p. (In Russ.)

30. Ferapontov N. B., Vdovina S. N., Gagarin A. N., Strusovskaja N. L., Tokmachev M. G. Water properties in hydrophylic polymer gels. *Kondensirovannye sredy i mezhfaznye granicy = Condensed Matter and Interphases*. 2011;13(2): 208–214. Available at: http://www.kcmf.vsu.ru/resources/t_13_2_2011_015.pdf (In Russ.)

31. Frenkel L. S. Nuclear magnetic resonance method for determining the moisture holding capacity of cation exchange resins as a function of temperature. *Analytical Chemistry*. 1973;45(8): 1570–1571. DOI: https://doi.org/10.1021/ac60330a052

32. Kargovsky A. V. Water clusters: structures and optical vibrational spectra. *Izvestiya VUZ. Applied nonlinear dynamics*. 2006;14(5): 110–119. DOI: https://doi.org/10.18500/0869-6632-2006-14-5-110-119 (In Russ., abstract in Eng.)

33. Eisenberg D., Kauzmann W. *The Structure and properties of water*. Oxford: Oxford University Press; 1969. 296 p.

34. Yu T., Zhang H., Cao H., Zheng G. Understanding the enhanced removal of Bi(III) using modified crystalline antimonic acids: creation of a transitional pyrochlore-type structure and the Sb(V)–Bi(III) interaction behaviors. *Chemical Engineering Journal*. 2019;360: 313–324. DOI: https://doi.org/10.1016/j.cej.2018.11.209

35. Nakamoto K. *Infrared and raman spectra of inorganic and coordination compounds: Part A: Theory and applications inorganic chemistry* (Sixth ed.). New York: John Wiley & Sons; 2009. 419 p. DOI: https://doi.org/10.1002/9780470405840

36. Birchall T., Sleight A. W. Oxidation states in vanadium antimonate ("$VSbO_4$"). *Inorganic chemistry*. 1976;15(4): 868–870. DOI: https://doi.org/10.1021/ic50158a026

37. Guerrero-Pérez M. O. V-containing mixed oxide catalysts for reduction – oxidation-based reactions with environmental applications: A short review. *Catalysts*. 2018;8(11): 564. DOI: https://doi.org/10.3390/catal8110564

38. Yaroslavtsev A. B., Kotov V. Yu. Proton mobility in hydrates of inorganic acids and acid salts. *Russian Chemical Bulletin*. 2002;51(4): 555–568.

39. Pauling, L. The nature of the chemical bond – an introduction to modern structural chemistry. (3rd Edition). New York: Cornell University Press, Ithaca; 1960.

Информация об авторах

Liliya Yu. Kovalenko, Senior Lecturer of the Department of Solid State Chemistry and Nanoprocesses, Chelyabinsk State University, Chelyabinsk, Russian Federation, e-mail: lkovalenko90@mail.ru. ORCID iD: https://orcid.org/0000-0002-9187-6934.

Vladimir A. Burmistrov, DSc in Physics and Mathematics, Professor, Dean of Chemical Department, Chelyabinsk State University, Chelyabinsk, Russian Federation; e-mail: burmistrov@csu.ru. ORCID iD: https://orcid.org/0000-0002-7862-6017.

Dmitrii A. Zakhar'evich, PhD in Physics and Mathematics, Associate Professor, Acting Dean of Physical Department, Chelyabinsk State University, Chelyabinsk, Russian Federation; e-mail: dmzah@csu.ru. ORCID iD: https://orcid.org/0000-0003-1184-9571.

All authors have read and approved the final manuscript.

Translated by Valentina Mittova.
Edited and proofread by Simon Cox.